TOXICOLOGICAL SCIENCES **82**, 545–554 (2004)
doi:10.1093/toxsci/kfh269
Advance Access publication September 1, 2004

Block of Neuronal Nicotinic Acetylcholine Receptors by Organophosphate Insecticides

Chantal J. G. M. Smulders,* Tjerk J. H. Bueters,† Silvia Vailati,‡ Regina G. D. M. van Kleef* and Henk P. M. Vijverberg*,[1]

*Institute for Risk Assessment Sciences, Utrecht University, NL-3508 TD Utrecht, The Netherlands; †TNO Prins Maurits Laboratory, NL-2280 AA Rijswijk, The Netherlands; and ‡CNR Center of Cellular and Molecular Pharmacology, University of Milano, I-20129 Milano, Italy

Received June 24, 2004; accepted August 25, 2004

Chronic and acute exposure to organophosphate (OP) pesticides may lead to persistent neurological and neurobehavioral effects, which cannot be explained by acetylcholinesterase (AChE) inhibition alone. It is suggested that other brain proteins are involved. Effects of commonly used organophosphate pesticides on rat neuronal α4β2 nicotinic acetylcholine receptors (nAChRs) expressed in *Xenopus laevis* oocytes have been investigated using the two-electrode voltage clamp technique. Several OP pesticides, *e.g.*, parathion-ethyl, chlorpyrifos and disulfoton, inhibited the ACh-induced ion current with potencies in the micromolar range. The potency of inhibition increased with increasing concentrations of the agonist ACh. Comparison of the potency of nAChR inhibition with the potency of AChE inhibition demonstrated that some OPs inhibit nAChRs more potently than AChE. Binding experiments on α4β2 nAChRs showed that the OPs noncompetitively interact with nAChRs. The inhibitory effects on nAChRs are adequately described and explained by a sequential two-step mechanism, in which rapidly reversible OP binding to a separate binding site leads to inhibition followed by a stabilization of the blocked state or receptor desensitization. It is concluded that OPs interact directly with neuronal α4β2 nAChRs to inhibit the agonist-induced response. This implicates that neuronal α4β2 nAChRs are additional targets for some OP pesticides.

Key Words: **organophosphate pesticides; neuronal nicotinic acetylcholine receptor; rat brain acetylcholinesterase; *Xenopus* oocytes; two-microelectrode voltage clamp.**

Acute toxic symptoms of organophosphate (OP) poisoning are generally caused by inhibition of the enzyme acetylcholinesterase (AChE, EC 3.1.1.7), which leads to accumulation of acetylcholine (ACh) (O'Malley 1997; Solberg and Belkin, 1997). In addition, acute poisoning with organophosphates may lead to a range of neurological sequelae. Several OP compounds, *e.g.*, mipafox, leptophos and diisopropylfluorophosphate (DFP), cause degeneration of long axons in the spinal cord and peripheral nerves, a syndrome known as organophosphate-induced delayed neuropathy (OPIDN) (Ehrich *et al*., 1994). It has been demonstrated that the neurodegeneration is associated with a decreased activity or inhibition of the enzyme neuropathy target esterase (Winrow *et al*., 2003). Other organophosphates, *e.g.*, fenthion and dimethoate are associated with the intermediate syndrome (Senanayake and Karalliedde, 1987). The syndrome occurs after recovery of cholinergic crisis but before the expected onset of OPIDN, and symptoms involved are muscle weakness and paralysis.

Studies on repeated low-level exposure to organophosphates of many occupational groups such as sheep dippers, pesticide sprayers, and farmers give equivocal results (for review see Ray and Richards, 2001). Some studies describe no adverse health effects or even indicate improvement of cognitive functions (Ivens *et al*., 1998). However, several studies describe a range of neurobehavioral and neuropsychiatric disorders after chronic OP exposure at levels that cause no symptoms of acute poisoning (Salvi *et al*., 2003; Stephens *et al*., 1995). Some of these OP pesticides, *e.g.*, chlorpyrifos, show different toxicology profiles depending on age and gender of the animals (Levin *et al*., 2002; Moser *et al*., 1998, 2000). However, these differences cannot be explained by a different sensitivity of AChE of the animals to these pesticides (Mortensen *et al*., 1998). It is clear that exposure to low-level doses of OP pesticides, as well as acute poisoning, can lead to several neurological and neurobehavioral changes, which cannot be accounted for on the basis of AChE inhibition alone. It has been suggested that other, more sensitive brain proteins are involved (Ray and Richards, 2001).

In addition to inhibition of AChE, several organophosphates also interact directly with receptors of the cholinergic system or modulate the receptor expression levels. A number of organophosphorous compounds, *e.g.*, the warfare agents VX and soman and the pesticide metabolites paraoxon and malaoxon, displace the agonist ^{3}H-*cis*-methyldioxolane from its binding site, suggesting that these compounds interact directly with rat M2 muscarinic ACh receptors (Bakry *et al*., 1988; Chaudhuri *et al*., 1993; Ward *et al*., 1993). Binding to the agonist site of M2 as well as M4 muscarinic ACh receptors is also observed for the pesticide metabolites chlorpyrifos oxon, paraoxon, and

[1] To whom correspondence should be addressed at Institute for Risk Assessment Sciences, Utrecht University, P.O. Box 80176, NL-3508 TD Utrecht, The Netherlands. Tel + 31 (30) 2535397. Fax + 31 (30) 2535077. E-mail: H.Vijverberg@iras.uu.nl.

methylparaoxon (Howard and Pope, 2002; van den Beukel *et al*., 1997). Apart from direct receptor interactions, the pesticides parathion and chlorpyrifos differentially upregulate and downregulate muscarinic ACh receptor expression in neonatal rats (Betancourt and Carr, 2004; Chaudhuri *et al*., 1993; Richardson and Chambers, 2004; Tang *et al*., 2003). Effects on nicotinic acetylcholine receptors (nAChRs) are also reported. Some organophosphates, *e.g.*, echothiophate, DFP, and VX, block the open channel of muscle type nAChRs and desensitize the receptor (Bakry *et al*., 1988; Eldefrawi *et al*., 1988; Rao *et al*., 1987; Tattersall 1990). The pesticides chlorpyrifos and parathion and their oxon metabolites were shown to inhibit the carbamylcholine-stimulated binding of ^{3}H-thienyl-cyclohexylpiperidine (TCP) to the open ion channel of *Torpedo* electric organ nAChRs, but enhanced TCP binding in the absence of agonist. In addition, the OPs enhanced the apparent affinity of the nAChRs to carbamylcholine, suggesting that they induce receptor desensitization (Katz *et al*., 1997). Chronic DFP treatment results in loss of hippocampal neuronal nAChRs (Stone *et al*., 2000). Although the effects of OP pesticides on muscarinic and muscle type nAChRs have been investigated extensively and are suggested to play a role in OP toxicity, the modulation of neuronal nAChR function by OP pesticides remains to be elucidated.

We have systematically investigated effects of a range of organophosphate pesticides on neuronal α4β2 nAChRs heterologously expressed in *Xenopus laevis* oocytes. From 21 organophosphates tested, the six compounds that were the more potent ones to inhibit nAChRs were selected. For these compounds the potencies for inhibition of the nAChRs were compared to the potencies for inhibition of rat brain AChE. In addition, receptor binding data and a kinetic analysis of the effects further elucidate the mechanism of action of OPs on neuronal nAChRs.

MATERIALS AND METHODS

Chemicals. ACh (acetylcholine chloride), collagenase type I, DMSO (dimethylsulfoxide; ACS reagent), MS-222 (3-amino benzoic acid ethyl ester, methane sulfonate salt), NaCl, and neomycin solution (10 mg neomycin/ml in 0.9% NaCl) were obtained from Sigma (St. Louis, MO). Acephate, azinphos-methyl, chlorpyrifos, diazinon, dibrom, dimefox, dimethoate, disulfoton, EPN (phenylphosphonothioic acid O-ethyl O-(4-nitrophenyl) ester), fenthion, leptophos, malaoxon, malathion, methamidophos, paraoxon-ethyl, parathion-ethyl, parathion-methyl, and phoxim were purchased from Riedel-de Haën (Seelze, Germany). Tri-*p*-tolyl-phosphate and tri-*p*-tolyl-phosphite were obtained from Acros Organics (Geel, Belgium). Echothiophate iodide was a kind gift from Wyeth (Hoofddorp, The Netherlands). $CaCl_2$ (1 M solution), $MgCl_2$ (1 M solution), ethanol (AnalaR, 99.7–100% v/v), $MgSO_4$, $NaHCO_3$, and NaOH were purchased from BDH Laboratory Supplies (Poole, England). $Ca(NO_3)_2$, HEPES, and KCl were from Merck (Darmstadt, Germany). For AChE assays acetylthiocholine iodide, 5,5′-dithio-*bis*-(2-nitro)benzoic acid, ethopropazine, Triton X-100, and EDTA (ethylenediamine tetraacetic acid) were from Sigma. NaCl, K_2HPO_4 and KH_2PO_4 were bought from Merck, and Tris (2-amino-2-(hydroxymethyl)-1,3-propanediol) was obtained from Boehringer (Mannheim, Germany).

Saline solutions for electrophysiology were prepared with distilled water, and solutions for AChE assays were prepared with Milli-Q filtered water (Millipore SA, Molsheim, France). Stock solutions (0.1 M) of azinphos-methyl, diazinon, dibrom, chlorpyrifos, disulfoton, EPN, fenthion, leptophos, malaoxon, malathion, methamidophos, paraoxon-ethyl, phoxim, tri-*p*-tolyl-phosphate, and tri-*p*-tolyl-phosphite were prepared in DMSO. Stock solutions (0.01 M) of acephate, dimefox, dimethoate, and echothiophate iodide were prepared in Milli-Q filtered water. Stock solutions (0.1 M and 1 M) of parathion-ethyl and parathion-methyl were prepared in ethanol. The final ethanol concentration in all experiments was $< 0.03\%$ (v/v), at which the ACh-induced ion currents were not affected. cDNAs of nicotinic receptor subunits ligated into the pSM plasmid vector containing the SV40 viral promoter were a kind gift from Dr. J. W. Patrick (Baylor College of Medicine, Houston, TX).

Brain AChE preparation. Male Wistar rats (~350 g, $n = 5$; Harlan, Horst, The Netherlands) were decapitated and the brains were removed. The tissue was homogenized (900 rpm, 10 % w/v homogenate) in ice-cold buffer containing 50 mM Tris, 1 M NaCl, 5 mM EDTA and 1 % (v/v) Triton X-100, pH 7.4 and subsequently centrifuged for 10 min at 36,000 × g in a Ti50 rotor at 4°C (L8-70; Beckman Coulter Inc., Fullerton, CA). The supernatant was kept on ice and used within 3 h. An aliquot was drawn to determine the protein content, which ranged from 30 to 37 mg/ml.

Brain AChE inhibition. The stock solutions of the AChE inhibitors were diluted in a phosphate buffer (8 mM KH_2PO_4 and 48 mM K_2HPO_4, pH 7.4) to obtain work standards containing 0.001 μM to 1 mM of the inhibitor. Then 25 μl aliquots of the work standard were added to 225 μl of brain homogenate. After incubation for 1 min at 37°C, 25 μl, samples were drawn, added to 250 μl ice-cold phosphate buffer, mixed, and rapidly frozen in liquid nitrogen. These samples were stored at −70°C until analysis. Thawed samples were appropriately diluted and were assayed in quadruplicate for AChE activity using a 96-well microplate modification of the Ellman method (Bueters *et al*., 2003). Ethopropazine (10 μM) was used as a specific inhibitor of butyrylcholinesterase.

Receptor expression in oocytes. Mature female *Xenopus laevis* frogs (AmRep, Breda, The Netherlands) were anesthetized by submersion in 0.2% MS-222, and some ovarian lobes were surgically removed. Experimental procedures involving animals were approved by a local ethical committee and were in accordance with Dutch law. Oocytes were defolliculated manually after treatment with collagenase type I (1.5 mg/ml calcium-free Barth's solution) for 1.5 h at room temperature. Plasmids coding for α4 and β2 subunits of rat neuronal nAChRs (Boulter *et al*., 1987) were dissolved in distilled water. Stock solutions containing α4 or β2 subunit cDNAs at a 1:1 molar ratio, were injected into the nuclei of stages V and VI oocytes within 8 h after harvesting, using a Drummond microinjector. Approximately 1 ng of each plasmid containing α or β cDNA was injected in a total injection volume of 18.4 nl/oocyte. After injection, the oocytes were incubated at 19°C in modified Barth's solution containing 88 mM NaCl, 1 mM KCl, 2.4 mM $NaHCO_3$, 0.3 mM $Ca(NO_3)_2$, 0.41 mM $CaCl_2$, 0.82 mM $MgSO_4$, 15 mM HEPES, and 50 μg/ml neomycin. Experiments were performed on oocytes after 3–6 days of incubation (Zwart and Vijverberg, 1997).

Electrophysiology. Oocytes were voltage clamped using two microelectrodes (0.5–2.5 MΩ) filled with 3 M KCl and a custom-built voltage clamp amplifier with high-voltage output stage (Zwart and Vijverberg, 1997). The external saline was clamped at ground potential by means of a virtual ground circuit using an Ag/AgCl reference electrode and a platinum black-covered platinum electrode for current passing. Membrane current was measured with a current-to-voltage converter incorporated into the virtual ground circuit. The membrane potential was held at −40 mV and all experiments were performed at room temperature (21°–23°C). Oocytes were placed in a piece of tubing (internal diameter 3 mm), which was continuously perfused with saline solution (115 mM NaCl, 2.5 mM KCl, 1 mM $CaCl_2$, 10 mM HEPES, pH 7.2 with NaOH) at a rate of approximately 20 ml/min. Aliquots of concentrated stock solutions of ACh in distilled water were added to the saline immediately before the experiments. Compounds were applied by switching between control and compound-containing saline with a servomotor-operated valve. The compounds were applied for 20 s during the 40 s ACh application. Agonist applications were

alternated by 5 min of superfusion with agonist-free saline to allow the receptors to recover completely from desensitization. To minimize adsorption of organophosphates in the superfusion system, glass reservoirs and Teflon (PTFE) tubing (4 × 6 mm, Rubber, Hilversum, The Netherlands) were used. Membrane currents were low-pass filtered (eight-pole Bessel; −3 dB at 0.3 kHz), digitized (12 bits, 1,024 samples/record), and stored on disk for off-line computer analysis (Zwart and Vijverberg, 1997).

Binding studies—preparation of oocyte homogenates. Batches of 50–80 frozen oocytes expressing rat α4β2 nAChRs were thawed and homogenized in a Potter homogenizer in an excess of buffer A (50 mM Tris-HCl pH 7, 120 mM NaCl, 5 mM KCl, 1 mM $MgCl_2$, 2.5 mM $CaCl_2$ and 2 mM phenylmethylsulfonyl fluoride), centrifuged for 60 min at 30,000 × g, and rinsed twice. The homogenates were resuspended in the same buffer containing 20 μg/ml of the protease inhibitors leupeptin, bestatin, pepstatin A, and aprotinin. Receptor expression ranged from 172 to 286 fmol/mg protein, which corresponds to an average nAChR density of 41 to 50 fmol/oocyte (44.3 ± 1.6; mean ± SEM, $n = 5$).

^{3}H-Epibatidine binding. Preliminary time course experiments were performed before saturation and competition analyses to determine the time required for ^{3}H-epibatidine to reach equilibrium with the α4β2 nAChRs. In the epibatidine saturation experiments, aliquots of oocyte homogenates were incubated overnight at 4°C with concentrations of ^{3}H-epibatidine ranging between 0.005 and 2.5 nM diluted in buffer A. Nonspecific binding was determined in parallel by means of incubation in the presence of 100 nM unlabeled epibatidine. At the end of the incubation, the samples were filtered on GFC filters pre-soaked in polyethylenimine through a Brandell apparatus, and the filters were counted in a β counter. To test the ability of parathion-ethyl and disulfoton to inhibit ^{3}H-epibatidine binding, parathion-ethyl and disulfoton were dissolved in DMSO and then diluted in buffer A just before use. Serial dilutions were pre-incubated for 30 min at room temperature with homogenates containing α4β2 nAChRs. Subsequently, a final concentration of 0.05 nM ^{3}H-epibatidine was added for overnight incubation at 4°C.

Data analysis. Amplitudes of ion currents were measured and normalized to the amplitude of ACh-induced control responses (100%) to adjust for differences in receptor expression levels between oocytes and for small variations in response amplitude over time. The percentage of inhibition of the ACh-induced ion current by the organophosphates was calculated from the quotient of the amplitude of the response after 20 s coapplication of the organophosphate and that of the control response at the same time point. Standard concentration-effect curves were fitted to the experimental data according the Hill equation:

$$E = 100/[1 + (C/IC_{50})^{nH}], \quad (1)$$

where E represents the percentage response, C the concentration organophosphate, IC_{50} the concentration that reduces the response by 50%, and n_H the Hill slope. Each inhibition curve was fitted to data obtained from a single experiment. The mean concentration-effect curves are drawn using the calculated mean estimated values of the IC_{50} and Hill slope from n experiments. All data are represented as mean ± SD of n oocytes or brains. GraphPad Prism software (version 3.00) was used to fit the data and to assess statistical significance.

Ligand-binding data. The experimental data obtained from the saturation binding experiments were analyzed by means of a nonlinear least-squares procedure using the LIGAND program (Gotti *et al*., 1998). The binding parameters were calculated by fitting the saturation data. An "extra sum of squares" F-test was performed by the LIGAND program to evaluate the different binding models statistically (*i.e.*, one-site vs. two-site models, comparison of the binding parameters, etc.). The K_i values were determined by means of LIGAND, using the data obtained from three independent competition experiments.

Kinetics and two-step model. The dual rate of inhibition and the apparently concentration-dependent kinetics of reversal of inhibition were interpreted as a two-step sequential chemical equilibrium between organophosphate and nicotinic receptor:

$$C + R \underset{k_{off}}{\overset{k_{on}}{\longleftrightarrow}} CR \underset{k_{-1}}{\overset{k_{+1}}{\longleftrightarrow}} CR^* \quad (2)$$

In the model R is the activated nAChR, C the OP molecule, CR is a rapidly reversible (low affinity) blocked state of the receptor, and CR^* is a slowly reversible (high affinity) blocked state. Note that the transition from CR to CR^* and vice versa occurs without binding or dissociation of the OP molecule. The first step is considered to be fast as compared to the second. Forward rate constants k_{on} ($M^{-1}\,s^{-1}$) and k_{+1} (s^{-1}) and backward rate constants k_{off} (s^{-1}) and k_{-1} (s^{-1}) were calculated from the following relations between the concentration of the organophosphate [C] and the observed rapid (k_{fast}) and slow (k_{slow}) components of the inhibitory effect (*e.g.*, Zhao *et al*., 1999):

$$k_{fast} = k_{off} + k_{on}[C] \quad (2a)$$

$$k_{slow} = k_{-1} + k_{+1}/(1 + K_{d,1}/[C]). \quad (2b)$$

Note that with $K_{d,1} = k_{off} / k_{on}$ and $K_{d,2} = k_{-1} / k_{+1}$ this accounts for a concentration-dependent inhibitory effect with an apparent affinity of:

$$K_{d,apparent} = K_{d,1}/(1 + 1/K_{d,2}). \quad (2c)$$

The apparent rate constants of inhibition (k_{fast} and k_{slow}) were obtained from fitting the inhibition of ion current with a dual exponential function using custom-designed software (Labview, National Instruments Corporation, Austin, TX).

RESULTS

Effects of Organophosphates on Rat α4β2 nAChRs

The effects of 0.1 μM and 10 μM of 21 organophosphates, *i.e.*, acephate, azinphos-methyl, chlorpyrifos, diazinon, dibrom, dimefox, dimethoate, disulfoton, echothiophate iodide, EPN, fenthion, leptophos, malaoxon, malathion, methamidophos, paraoxon-ethyl, parathion-ethyl, parathion-methyl, phoxim, tri-*p*-tolyl-phosphate, and tri-*p*-tolyl-phosphite, on ion currents evoked by 1 μM ACh on rat α4β2 neuronal nAChRs have been investigated. The organophosphate pesticides were coapplied with ACh during the ACh-evoked response in order to assess possible potentiating or inhibitory actions. The organophosphates acephate, azinphos-methyl, diazinon, dibrom, dimefox, dimethoate, echothiophate iodide, leptophos, malaoxon, malathion, methamidophos, paraoxon-ethyl, phoxim, tri-*p*-tolyl-phosphate, and tri-*p*-tolyl-phosphite produced <3% effect at a concentration of 0.1 μM and <15% effect at 10 μM (data not shown).

Chlorpyrifos, disulfoton, EPN, fenthion, parathion-ethyl, and parathion-methyl inhibited the ACh-induced ion current substantially. For all of these compounds, inhibition of the 1 μM ACh-induced ion current was less than the inhibition of the 1 mM ACh-induced ion current (Fig. 1). The concentration-dependent effects of chlorpyrifos, disulfoton, EPN, fenthion, parathion-ethyl, and parathion-methyl at 1 μM ACh and 1 mM ACh were investigated in detail, as shown for the inhibition of the 1 mM ACh-induced ion current by disulfoton in Figure 2. The kinetics of the responses in Figure 2 illustrate that the rate of

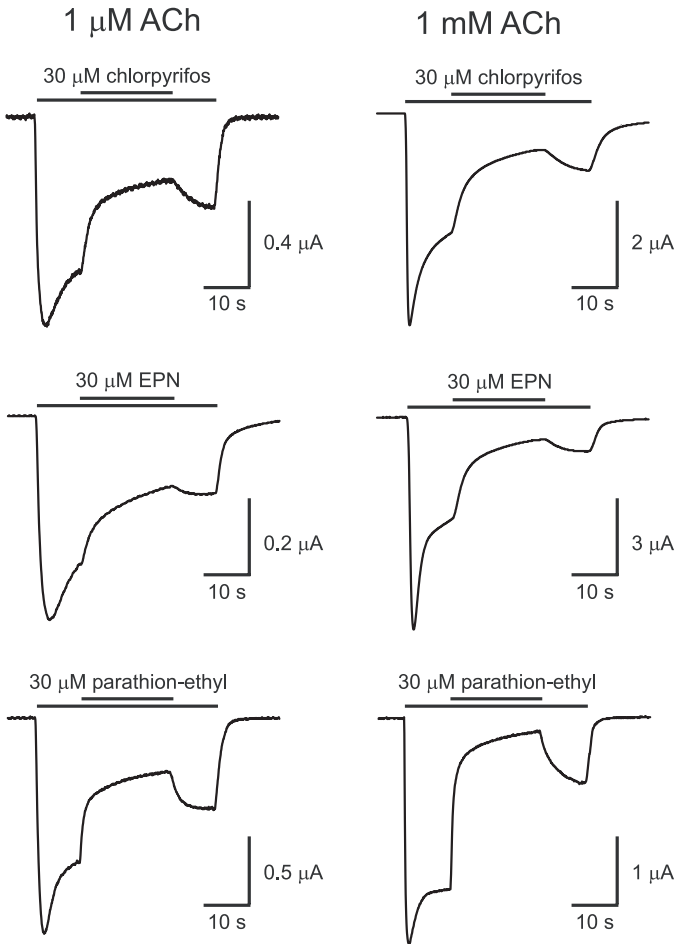

FIG. 1. Inhibitory effects of 30 μM of the OP pesticides chlorpyrifos, EPN, and parathion-ethyl on 1 μM and 1 mM ACh-induced ion currents mediated by α4β2 nAChRs expressed in *Xenopus* oocytes. The horizontal bars on top of the traces indicate the period of superfusion with external solution containing ACh and OP at the concentrations indicated. The OPs were applied for 20 s during the 40 s ACh application. Note that the OPs inhibit 1 mM ACh-induced ion currents more potently than ion currents induced by 1 μM ACh.

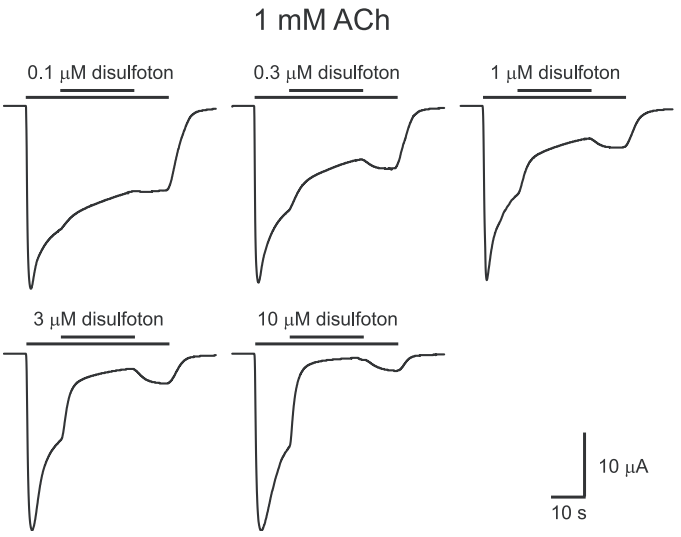

FIG. 2. Concentration-dependent inhibition of ion currents evoked by 1 mM ACh by disulfoton. The horizontal bars on top of the traces indicate the period of superfusion with external solution containing 1 mM ACh and disulfoton at increasing concentrations as indicated. After application of high concentrations disulfoton (*i.e.*, ≥ 3 μM) the response did not fully recover upon wash-out of the OP. The scale bar applies to all traces, which were from the same oocyte.

onset of inhibition increased with the concentration of organophosphate. At wash-out of the organophosphate, the reverse was observed. The rate of recovery of the ACh-induced ion current decreased with the concentration of organophosphate. On the wash-out of high concentrations of organophosphates the ACh-induced ion current did not fully recover before termination of the superfusion with ACh.

The concentration dependence of inhibition by disulfoton, fenthion, parathion-ethyl, and parathion-methyl was assessed at agonist concentrations of 1 μM ACh and 1 mM ACh (Fig. 3). Coapplication of the solvent DMSO at concentrations up to 0.1% (v/v) with ACh did not result in detectable effects. Marginal inhibitory effects were observed for 0.3% and 1% DMSO, *i.e.*, solvent concentrations associated with the organophosphate concentrations of 0.3 mM and 1 mM, respectively. Because of solubility problems, it was not possible to obtain complete concentration-effect curves for chlorpyrifos and EPN. For the same reason, data points of 0.3 mM disulfoton, fenthion, parathion-ethyl, and parathion-methyl were omitted from the curve fit. Disulfoton, fenthion, parathion-ethyl, and parathion-methyl inhibited 1 μM ACh induced ion currents with potencies ranging from 7 μM for disulfoton to 75 μM for fenthion (Table 1). The potency order is disulfoton $>$ parathion-ethyl, parathion-methyl $>$ fenthion. For all organophosphates, a clear left-shift of the inhibition curves is observed when the agonist concentration is raised from 1 μM to 1 mM (Fig. 3; Table 1). Approximate IC_{50} values of chlorpyrifos and EPN to inhibit the 1 mM ACh-induced ion current were in the range of 3–30 μM and 10–100 μM, respectively.

Effects of Organophosphates on Rat Brain AChE

The inhibitory effects of the different organophosphate pesticides on rat brain AChE activity were also determined for comparison with the effects on the nAChR demonstrated here. Rat brain homogenate was incubated with increasing concentrations of the organophosphates chlorpyrifos, disulfoton, EPN, fenthion, parathion-ethyl, and parathion-methyl. The concentrations of the compounds ranged from 10 nM to 1 mM. The solvent DMSO, at the maximum final concentration of 1% (v/v) in these experiments, did not noticeably affect the rat brain AChE activity. The concentration-dependent reduction of rat brain AChE activity by the organophosphates is shown in Figure 4. Concentration-effect curves were fitted to the data according to the Hill equation. Disulfoton, EPN, and fenthion

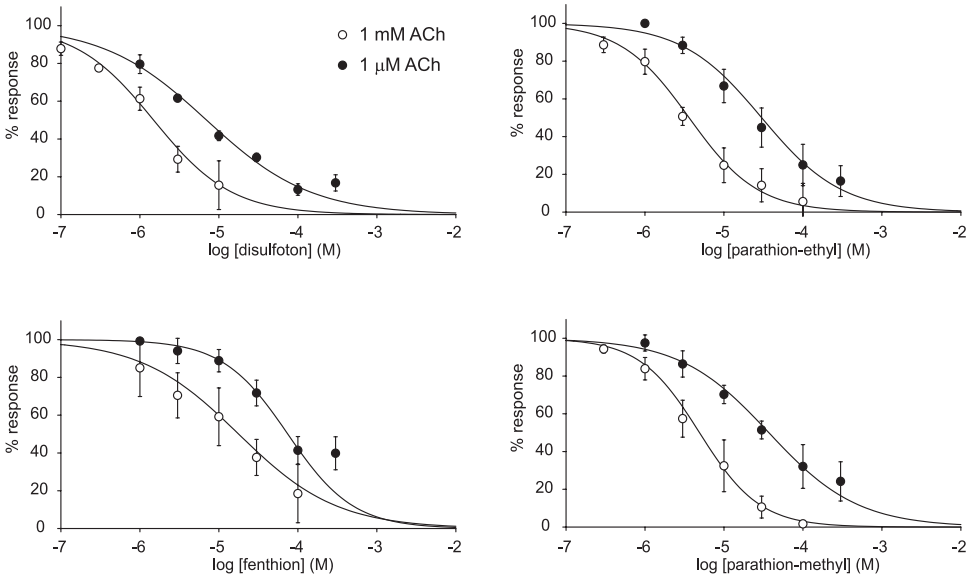

FIG. 3. Concentration-effect curves for the inhibition of l μM ACh- (solid circles) and 1 mM ACh-evoked (open circles) ion current by disulfoton, fenthion, parathion-ethyl, and parathion-methyl. The data are depicted as mean ± SD. Error bars smaller than the size of the symbols are not shown. The lines are drawn according to the mean parameters of 3–4 inhibition curves fitted to data from different oocytes. Estimated values of IC_{50} and n_H are shown in Table 1.

TABLE 1
Pharmacological Parameters of nAChR Inhibition and nAChR Binding by OPs

	1 μM ACh IC_{50} (μM)	n_H	1 mM ACh IC_{50} (μM)	n_H	Binding K_i (mM)
disulfoton	7.0 ± 1.5	0.66 ± 0.01	1.5 ± 0.5	0.88 ± 0.19	>100
fenthion	74.6 ± 20.3	1.05 ± 0.11	17.8 ± 14.2	0.70 ± 0.14	n.d.
parathion-ethyl	30.1 ± 14.8	0.86 ± 0.18	3.6 ± 0.7	1.00 ± 0.36	>100
parathion-methyl	37.0 ± 13.0	0.77 ± 0.09	4.9 ± 2.3	1.14 ± 0.06	n.d.

Note. All values are mean ± SD of the parameters of concentration-effect curves fitted to the data obtained from 3–4 oocytes.

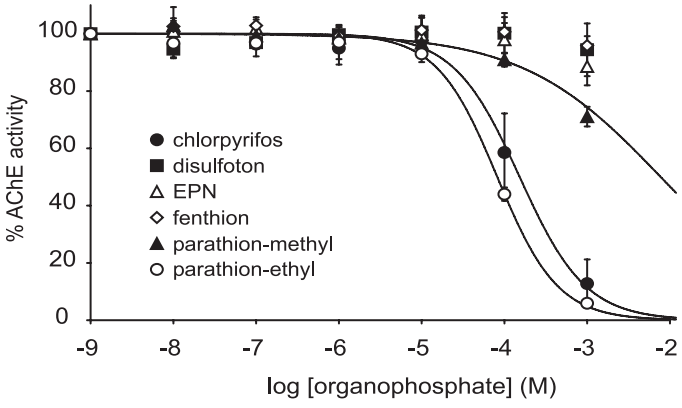

FIG. 4. The concentration-dependent inhibition of rat brain AChE by the OP pesticides chlorpyrifos, disulfoton, EPN, fenthion, parathion-ethyl, and parathion-methyl. The data are depicted as mean ± SD. Error bars smaller than the size of the symbols are not shown. The drawn lines are the mean inhibition curves obtained from 4–5 independent experiments. Estimated values of IC_{50} and n_H are given in Table 2.

TABLE 2
AChE Inhibition by OP Pesticides

	IC_{50} (μM)	n_H
Chlorpyrifos	153 ± 88	1.09 ± 0.18
Disulfoton	>1,000	—
EPN	>1,000	—
Fenthion	>1,000	—
Parathion-ethyl	82 ± 6	1.19 ± 0.13
Parathion-methyl	>1,000	—

Note. Values are mean ± SD of the parameters of concentration-effect curves fitted to the data obtained from 4–5 independent experiments.

up to concentrations of 1 mM did not cause a marked reduction of the AChE activity. Parathion-methyl inhibited the AChE activity at concentrations ≥100 μM. The low potency of parathion-methyl precluded the fitting of inhibition curves and the estimation of the IC_{50} value, which was well beyond

1 mM. Chlorpyrifos and parathion-ethyl inhibited the rat brain AChE activity virtually completely, with IC_{50} values of 153 ± 88 μM and 82 ± 7 μM, respectively. The potency order for rat brain AChE inhibition by the organophosphates is parathion-ethyl > chlorpyrifos ≫ parathion-methyl > disulfoton, EPN, fenthion (Fig. 4).

Competition Binding of Disulfoton and Parathion-ethyl with ^{3}H-epibatidine

The dependence of the inhibitory effects of the organophosphate pesticides on agonist concentration might indicate that both interact with the same sites on the nAChR. Therefore, experiments have been performed on membranes of oocytes transfected with rat α4β2 nAChRs to investigate possible competition between the binding of disulfoton and parathion-ethyl and that of ^{3}H-epibatidine, a radiolabeled agonist of the nAChR. Saturation binding (Fig. 5A) yielded a K_d of 46 pM ^{3}H-epibatidine (coefficient of variation 11%) and a B_{max} of 237 ± 30 fmol/mg protein (mean ± SEM, $n = 5$). The binding data were analyzed for a single vs. two-site interaction, but there was no statistical better fit for the two-site model. Nonspecific binding, determined in parallel by means of incubation in the presence of unlabeled epibatidine, amounted to 5–15% of total binding. Analysis of the specific binding data yielded linear Scatchard plots, demonstrating the presence of a single class of high-affinity epibatidine binding sites in membranes of oocytes transfected with rat α4β2 nAChRs. No specific ^{3}H-epibatidine binding was found in membranes prepared from untransfected oocytes.

Specific ^{3}H-epibatidine binding to oocyte homogenates showed no significant displacement by the organophosphates up to concentrations of 10 mM (Fig. 5B). The K_i values for disulfoton and parathion-ethyl estimated from the displacement experiments were >100 mM. Similar experiments with ACh yielded a K_i value for the displacement of ^{3}H-epibatidine by ACh of 39 nM (coefficient of variation 13%). These results show that the agonist epibatidine bound to the agonist recognition sites of rat α4β2 nAChRs is neither displaced by disulfoton nor by parathion-ethyl.

Noncompetitive Mechanisms

The binding experiments demonstrate that the inhibition of the ACh-induced ion current by the organophosphates disulfoton and parathion-ethyl is due to noncompetitive effects. Therefore, various possibilities for noncompetitive inhibition of the neuronal type nAChR by the organophosphates have been investigated. To assess whether the organophosphate itself is the agent causing the inhibitory effect, experiments were performed in which ACh and parathion-ethyl were coapplied and subsequently washed out, each separately or both together. The result shows a rebound tail current indicating reversal of block only when parathion-ethyl is washed out (Fig. 6A). On wash-out of ACh, the remaining inward current rapidly declined to zero irrespective of whether parathion-ethyl remained present or not and rebound tail currents were not observed. These results show that parathion-ethyl blocks the ion current and rules out the possibility that the inhibitory effect is caused by an enhancement of the channel blocking potency of ACh in the presence of parathion-ethyl.

The possible alternatives of open and closed channel block were also evaluated. The results in Figure 6B show that parathion-ethyl at a concentration that causes nearly complete block when applied during the ACh-induced response also causes a strong inhibitory effect when applied

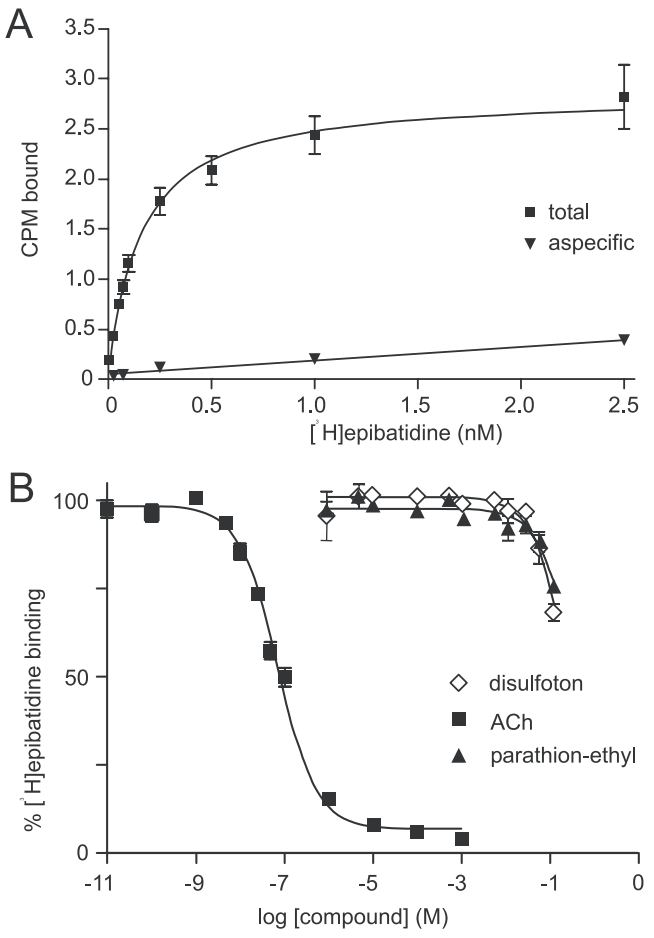

FIG. 5. Competition binding of disulfoton and parathion-ethyl with ^{3}H-epibatidine in homogenates of oocytes expressing rat α4β2 nAChRs. (A) Saturation curve of ^{3}H-epibatidine binding. For the total binding the oocyte homogenate was incubated with the indicated concentration of ^{3}H-epibatidine. Nonspecific binding was determined in the presence of 100 nM unlabeled epibatidine. Data are mean ± SEM values from three experiments, each performed in duplicate. (B) Displacement of bound ^{3}H-epibatidine by ACh, disulfoton, and parathion-ethyl. Oocyte homogenate was preincubated with the indicated concentration of disulfoton and parathion-ethyl for 30 min and then 0.05 nM ^{3}H-epibatidine was added and the samples were incubated overnight at 4°C. Data are mean ± SEM values of four experiments, each performed in duplicate.

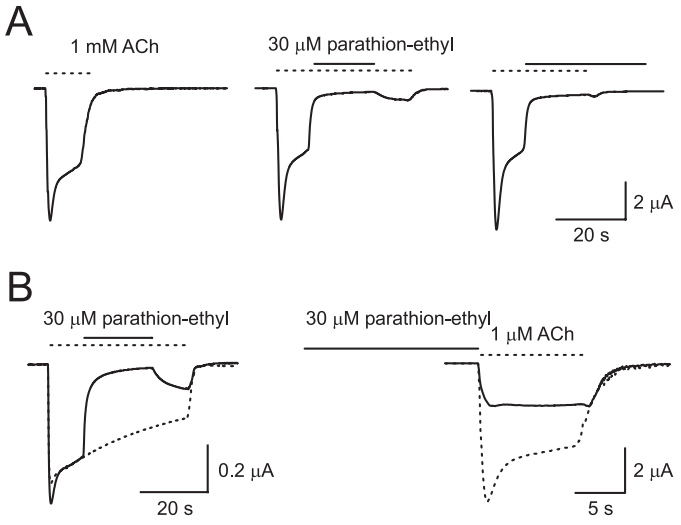

FIG. 6. The mechanism of noncompetitive inhibition of rat α4β2 nAChRs expressed in *Xenopus* oocytes by parathion-ethyl. (A) The ion current evoked by 1 mM ACh rapidly declines when the agonist is washed out (left panel). After coapplication of 30 μM parathion-ethyl and 1 mM ACh to the same oocyte, a rebound tail current, indicating reversal of inhibition, is observed when parathion-ethyl is washed out in the presence of ACh (middle panel). On wash-out of ACh in the presence of parathion-ethyl, the remaining current rapidly declines to baseline level (right panel). This indicates that parathion-ethyl alone is the agent causing the inhibitory effect. (B) Application of 30 μM parathion-ethyl for a period of 20 s immediately prior to the application of 1 μM ACh in an oocyte expressing α4β2 nAChRs causes extensive inhibition (right panel) as the coapplication of the two compounds to the same oocyte for the same period (left panel). This shows that inhibition by parathion-ethyl occurs in the absence of ACh, *i.e.*, when the ligand-gated ion channels are closed. Horizontal bars indicate the periods of application of ACh (dashed bars) and parathion-ethyl (solid bars) at the concentrations indicated.

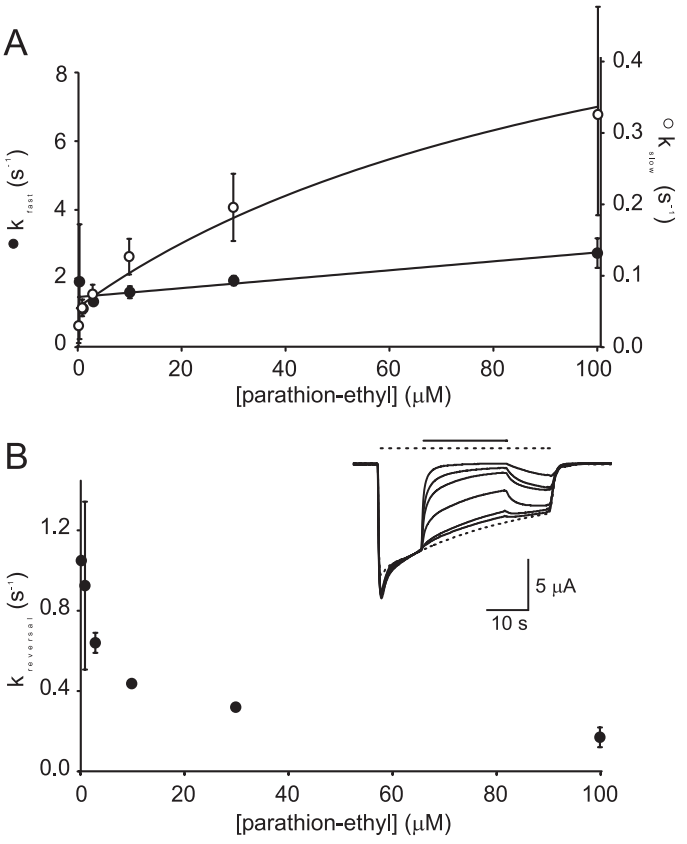

FIG. 7. Kinetics of inhibition of rat α4β2 nAChR-mediated ion current by parathion-ethyl. (A) The onset of inhibition shows a dual exponential decay. The data points (mean ± SD, $n = 3$) are the rate constants obtained from a dual exponential fit to current traces as in the inset in B. The drawn lines in A are eq. (2a) and eq. (2b) fitting the relation between the rate constants k_{fast} (filled circles) and k_{slow} (open circles) and parathion-ethyl concentration. The superimposed traces (inset B) represent the increasing inhibitory effects of 0.3, 1, 3, 10, 30, and 100 μM parathion-ethyl superfused for 20 s during the 1 mM ACh-induced response. (B) The reversal of inhibition after 20 s of superfusion with parathion-ethyl and ACh on switching to saline containing ACh only (see inset). The rate of reversal of the inhibitory effect, obtained from fitting a single exponential function to the traces as in the inset, decreased with increasing inhibition by increasing concentrations of parathion-ethyl.

before application of ACh. These results demonstrate that the presence of the agonist is not required for the inhibitory effect to occur and that open channel block cannot account for the noncompetitive, inhibitory effect of parathion-ethyl.

Onset and Reversal of Inhibition

The kinetics of the effects of parathion-ethyl show that the rate of onset of inhibition increased with organophosphate concentration (Fig. 7A). Values of the apparent fast and slow rate constants of the onset of inhibition were obtained by fitting eq. (3) to the data as shown in the inset of Figure 7A and plotted against parathion-ethyl concentration. An inverse relation between organophosphate concentration and the rate of reversal of inhibition was obtained on wash-out (Fig. 7B). The rate of reversal of inhibition of the ACh-induced ion current decreased with increasing concentration of parathion-ethyl. After administration of high concentrations of organophosphates, the inhibitory effect did not fully reverse on wash-out of the organophosphate within the period until the termination of superfusion with ACh (Fig. 7 inset). The features of inhibition are consistent with a sequential model as shown in equation (2). Regression lines according to eq. (2a) and eq. (2b) in Figure 7A show an approximate compliance of the effects observed with the two-step sequential mechanism of equation (2). The rate constants obtained from the regressions are: $k_{on} = 0.013\ \mu M^{-1}s^{-1}$, $k_{off} = 1.45\ s^{-1}$ ($K_{d,1} = 112\ \mu M$), and $k_{+1} = 0.60\ s^{-1}$, $k_{-1} = 0.057\ s^{-1}$ ($K_{d,2} = 0.10$), and the apparent affinity of the overall process of inhibition by parathion-ethyl, according to eq. (2c), $K_{d,apparent} = 9.8\ \mu M$. For disulfoton rate constants obtained are: $k_{on} = 0.046\ \mu M^{-1}s^{-1}$, $k_{off} = 0.48\ s^{-1}$, ($K_{d,1} = 10\ \mu M$), $k_{+1} = 0.23\ s^{-1}$, and $k_{-1} = 0.021\ s^{-1}$, ($K_{d,2} = 0.09$) resulting in an apparent affinity for disulfoton of 0.85 μM. These values are within the same order of magnitude as the IC_{50} values of the inhibition curves of parathion-ethyl and disulfoton (Table 1).

DISCUSSION

The results demonstrate that several organophosphate pesticides inhibit ACh-induced ion currents in *Xenopus laevis* oocytes transfected with rat neuronal α4β2 nAChRs with micromolar potencies. The absence of effects of malaoxon and paraoxon-ethyl indicates that the effects on neuronal α4β2 type nAChRs are associated with the ''thio-'' form and not the ''oxon-'' form of the organophosphates. Conversely, muscarinic M2 type ACh receptors have been reported to have a higher affinity for the ''oxon'' as compared to the ''thio-'' form of some OP pesticides (Howard and Pope, 2002; Ward *et al*., 1993).

The organophosphates tested have a wide range of inhibitory potencies. For the inhibition of nAChRs, the more potent pesticides, in order of potency, were disulfoton > parathion-ethyl, parathion-methyl > fenthion. The inhibitory effects are more potent at high concentrations of ACh than at low concentrations of the agonist (Fig. 3). For six organophosphates, that were shown to inhibit α4β2 nAChRs, the potencies for inhibition of rat brain AChE were determined: chlorpyrifos and parathion-ethyl significantly inhibited AChE activity, whereas parathion-methyl, fenthion, EPN, and disulfoton did not. This was expected, because most organophosphates need to be metabolized to their active oxons to cause potent AChE inhibition; *e.g.*, reported values of the IC_{50} of inhibition of rat brain cholinesterase are 3–5 nM for paraoxon and 35–36 nM for malaoxon (Ward *et al*., 1993). Theoretically, the first effect of exposure to an organophosphate may consist of impairment of cholinergic transmission resulting from nAChR inhibition. After formation of the active metabolites, AChE will be inhibited, resulting in an increase of ACh in the synaptic cleft (Soreq and Seidman, 2001). The elevated concentration of ACh will, at the same time, cause an increase of nAChR activation and enhance the inhibitory effect of the organophosphates on the nAChRs. Thus the stimulating effects of AChE inhibition on nicotinic neurotransmission are counteracted by an enhanced potency of inhibition of nAChRs by the organophosphates. In practice, symptoms related to inhibition of AChE may prevail, even for poisoning by the ''thio'' OP compounds, because of the much higher potency of the oxon metabolites for inhibition of AChE. Kinetic studies with chlorpyrifos have shown that AChE inhibition in plasma occurs within minutes and changes over hours after oral dosing (Timchalk *et al*., 2002), indicating that the oxon metabolite is rapidly formed. Thus, the main effect of the interaction of the parent compound with the nAChR may be to postpone the symptoms of AChE inhibition. A carefully designed study would be required to investigate the various possibilities and to distinguish between symptoms specifically related to effects of OP compounds on AChE and on muscarinic and nicotinic AChR.

Although the mechanisms of AChE inhibition have been described in detail (Soreq and Seidman, 2001), the nature of the inhibitory effect of the organophosphate pesticides on nicotinic ACh receptors is less evident. Competition binding experiments demonstrate that the organophosphates parathion-ethyl and disulfoton at concentrations ≤10 mM do not bind to the agonist-recognition site of rat α4β2 nAChRs (Fig. 5). This demonstrates that a noncompetitive mechanism is responsible for the inhibitory effect of the organophosphate on the nAChR-mediated ion current. Because parathion-ethyl can inhibit the α4β2 nAChRs in the absence of ACh (Fig. 6), it is concluded that channel opening is not required for the inhibitory effect. The biphasic kinetics of onset of inhibition and the concentration-dependence of the kinetics of reversal of inhibition (Fig. 7) suggest that the ion current is inhibited by a two-step mechanism. Fitting a sequential two-step equilibrium, with a rapidly reversible association and dissociation of the organophosphate followed by a slowly reversible transition (Zhao *et al*., 1999), to the inhibitory effects of parathion-ethyl and disulfoton (Fig. 7) yielded potencies of the OPs comparable to those obtained from the inhibition curves (Fig. 3). The kinetics of reversal of inhibition are inversely related to OP concentration. This finding is similar to what has been reported before for the inhibition of human muscle type nAChRs in TE-671 cells by the philanthotoxin PhTX-(12). PhTX-(12) is a weak open channel blocker and is supposed to enhance receptor desensitization (Brier *et al*., 2003). In addition, it has been suggested that the noncompetitive interaction of chlorpyrifos and parathion and their oxons with muscle nAChRs also leads to receptor desensitization (Katz *et al*., 1997). Based on these and the present results, it is more likely that the secondary blocked state in our model (eq. 2) represents a desensitized state rather than a blocked state, because enhancement of desensitization would also account for the enhanced potency of parathion-ethyl and disulfoton at elevated ACh concentration (Fig. 3).

The toxicological relevance of effects of OP pesticides on neuronal nAChRs lies in the fact that a number of neurotoxic symptoms cannot be accounted for on the basis of AChE inhibition alone. Although the effects of desensitization of α4β2 nAChRs are still unclear, some indication of effects to be expected can be derived from studies on knockout mice. Mice lacking the α4 nAChR subunit display a reduced antinociceptive effect of nicotine (Marubio *et al*., 1999) and elevated anxiety (Ross *et al*., 2000). Knock-out of the β2 nAChR subunit demonstrated that the β2 subunit is involved in the reinforcing properties of nicotine (Picciotto *et al*., 1998) and in passive avoidance learning (Cordero-Erausquin *et al*., 2000). Thus, chronic or repeated desensitization of α4β2 nAChRs might result in several neurological and neurobehavioral deficits. In this respect, it is remarkable that in farmers chronically exposed to OP pesticides, increased anxiety is one of the more frequently diagnosed symptoms (Salvi *et al*., 2003).

In conclusion, a number of OP pesticides have been demonstrated to interact directly with neuronal α4β2 nAChRs to inhibit the ACh-induced response in a noncompetitive way. The inhibition is accounted for by a two-step mechanism resulting in receptor desensitization. The results indicate that neuronal AChRs constitute additional targets for the effects of OPs on the nervous system.

ACKNOWLEDGMENTS

We thank Dr. Jim Patrick (Baylor College of Medicine, Houston, TX) for the gift of the cDNA clones of nAChR subunits, Dr. Cecilia Gotti for help with the binding experiments, Ing. Aart de Groot for development of the analysis program and assistance with the data analysis, Bas Koomen for taking care of the frogs, and Wyeth, The Netherlands, for the gift of echothiophate.

REFERENCES

Bakry, N. M., el-Rashidy, A. H., Eldefrawi, A. T., and Eldefrawi, M. E. (1988). Direct actions of organophosphate anticholinesterases on nicotinic and muscarinic acetylcholine receptors. *J. Biochem. Toxicol.* **3,** 235–259.

Betancourt, A. M., and Carr, R. L. (2004). The effect of chlorpyrifos and chlorpyrifos-oxon on brain cholinesterase, muscarinic receptor binding, and neurotrophin levels in rats following early postnatal exposure. *Toxicol. Sci.* **77,** 63–71.

Boulter, J., Connolly, J., Deneris, E., Goldman, D., Heinemann, S., and Patrick, J. (1987). Functional expression of two neuronal nicotinic acetylcholine receptors from cDNA clones identifies a gene family. *Proc. Natl. Acad. Sci. U.S.A.* **84,** 7763–7767.

Brier, T. J., Mellor, I. R., Tikhonov, D. B., Neagoe, I., Shao, Z., Brierley, M.T., Strømgaard, K., Jaroszewski, J. W., Krogsgaard-Larsen, P., and Usherwood, P. N. R. (2003). Contrasting actions of philanthotoxin-343 and philanthotoxin-(12) on human muscle nicotinic acetylcholine receptors. *Mol. Pharmacol.* **64,** 954–964.

Bueters, T. J., Joosen, M. J., Van Helden, H. P., Ijzerman, A. P. and Danhof, M. (2003). Adenosine A(1) receptor agonist N(6)-cyclopentyladenosine affects the inactivation of acetylcholinesterase in blood and brain by sarin. *J. Pharmacol. Exp. Ther.* **304,** 1307–1313.

Chaudhuri, J., Chakraborti, T. K., Chanda, S., and Pope, C. N. (1993). Differential modulation of organophosphate-sensitive muscarinic receptors in rat brain by parathion and chlorpyrifos. *J. Biochem. Toxicol.* **8,** 207–216.

Cordero-Erausquin, M., Marubio, L. M., Klink, R., and Changeux, J. P. (2000). Nicotinic receptor function: New perspectives from knockout mice. *Trends Pharmacol. Sci.* **21,** 211–217.

Ehrich, M., Correll, L., and Veronesi, B. (1994). Neuropathy target esterase inhibition by organophosphorus esters in human neuroblastoma cells. *Neurotoxicology* **15,** 309–313.

Eldefrawi, M. E., Schweizer, G., Bakry, N. M., and Valdes, J. J. (1988). Desensitization of the nicotinic acetylcholine receptor by diisopropylfluorophosphate. *J. Biochem. Toxicol.* **3,** 21–32.

Gotti, C., Balestra, B., Moretti, M., Rovati, G. E., Maggi, L., Rossoni, G., Berti, F., Villa, L., Pallavicini, M., and Clementi, F. (1998). 4-Oxystilbene compounds are selective ligands for neuronal nicotinic α-bungarotoxin receptors. *Br. J. Pharmacol.* **124,** 1197–1206.

Howard, M. D., and Pope, C. N. (2002). In vitro effects of chlorpyrifos, parathion, methyl parathion and their oxons on cardiac muscarinic receptor binding in neonatal and adult rats. *Toxicology* **170,** 1–10.

Ivens, I. A., Schmuck, G., and Machemer, L. (1998). Learning and memory of rats after long-term administration of low doses of parathion. *Toxicol. Sci.* **46,** 101–111.

Katz, E. J., Cortes, V. I., Eldefrawi, M. E., and Eldefrawi, A. T. (1997). Chlorpyrifos, parathion, and their oxons bind to and desensitize a nicotinic acetylcholine receptor: Relevance to their toxicities. *Toxicol. Appl. Pharmacol.* **146,** 227–236.

Levin, E. D., Addy, N., Baruah, A., Elias, A., Christopher, N. C., Seidler, F. J., and Slotkin, T. A. (2002). Prenatal chlorpyrifos exposure in rats causes persistent behavioral alterations. *Neurotoxicol. Teratol.* **24,** 733–741.

Marubio, L. M., del Mar Arroyo-Jimenez, M., Cordero-Erausquin, M., Léna, C., Le Novère, N., de Kerchove d'Exaerde, A., Huchet, M., Damaj, M. I., and Changeux, J. P. (1999). Reduced antinociception in mice lacking neuronal nicotinic receptor subunits. *Nature* **398,** 805–810.

Mortensen, S. R., Hooper, M. J., and Padilla, S. (1998). Rat brain acetylcholinesterase activity: Developmental profile and maturational sensitivity to carbamate and organophosphorus inhibitors. *Toxicology* **125,** 13–19.

Moser, V. C., Chanda, S. M., Mortensen, S. R., and Padilla, S. (1998). Age- and gender-related differences in sensitivity to chlorpyrifos in the rat reflect developmental profiles of esterase activities. *Toxicol. Sci.* **46,** 211–222.

Moser, V. C. (2000). Dose-response and time-course of neurobehavioral changes following oral chlorpyrifos in rats of different ages. *Neurotoxicol. Teratol.* **22,** 713–723.

O'Malley, M. (1997). Clinical evaluation of pesticide exposure and poisonings. *Lancet* **349,** 1161–1166.

Picciotto, M. R., Zoli, M., Rimondini, R., Léna, C., Marubio, L. M., Pich, E. M., Fuxe, K., and Changeux, J. P. (1998). Acetylcholine receptors containing the beta2 subunit are involved in the reinforcing properties of nicotine. *Nature* **391,** 173–177.

Rao, K. S., Aracava, Y., Rickett, D. L., and Albuquerque, E. X. (1987). Noncompetitive blockade of the nicotinic acetylcholine receptor-ion channel complex by an irreversible cholinesterase inhibitor. *J. Pharmacol. Exp. Ther.* **240,** 337–344.

Ray, D. E., and Richards, P. G. (2001). The potential for toxic effects of chronic, low-dose exposure to organophosphates. *Toxicol. Lett.* **120,** 343–351.

Richardson, J. R., and Chambers, J. E. (2004). Neurochemical effects of repeated gestational exposure to chlorpyrifos in developing rats. *Toxicol. Sci.* **77,** 83–90.

Ross, S. A., Wong, J. Y., Clifford, J. J., Kinsella, A., Massalas, J. S., Horne, M. K., Scheffer, I. E., Kola, I., Waddington, J. L., Berkovic, S. F., and Drago, J. (2000). Phenotypic characterization of an alpha 4 neuronal nicotinic acetylcholine receptor subunit knock-out mouse. *J. Neurosci.* **20,** 6431–6441.

Salvi, R. M., Lara, D. R., Ghisolfi, E. S., Portela, L. V., Dias, R. D., and Souza, D. O. (2003). Neuropsychiatric evaluation in subjects chronically exposed to organophosphate pesticides. *Toxicol. Sci.* **72,** 267–271.

Senanayake, N., and Karalliedde, L. (1987). Neurotoxic effects of organophosphorus insecticides. An intermediate syndrome. *N. Engl. J. Med.* **316,** 761–763.

Solberg, Y., and Belkin, M. (1997). The role of excitotoxicity in organophosphorous nerve agents central poisoning. *Trends Pharmacol. Sci.* **18,** 183–185.

Soreq, H., and Seidman, S. (2001). Acetylcholinesterase—New roles for an old actor. *Nat. Rev. Neurosci.* **2,** 294–302.

Stephens, R., Spurgeon, A., Calvert, I. A., Beach, J., Levy, L. S., Berry, H., and Harrington, J. M. (1995). Neuropsychological effects of long-term exposure to organophosphates in sheep dip. *Lancet* **345,** 1135–1139.

Stone, J. D., Terry, A. V., Pauly, J. R., Prendergast, M. A., and Buccafusco, J. J. (2000). Protractive effects of chronic treatment with an acutely sub-toxic regimen of diisopropylfluorophosphate on the expression of cholinergic receptor densities in rats. *Brain Res.* **882,** 9–18.

Tang, J., Carr, R. L., and Chambers, J. E. (2003). The effects of repeated oral exposures to methyl parathion on rat brain cholinesterase and muscarinic receptors during postnatal development. *Toxicol. Sci.* **76,** 400–406.

Tattersall, J. E. (1990). Effects of organophosphorus anticholinesterases on nicotinic receptor ion channels at adult mouse muscle endplates. *Br. J. Pharmacol.* **101,** 349–357.

Timchalk, C., Nolan, R. J., Mendrala, A. L., Dittenber, D. A., Brzak, K. A., and Mattsson, J. L. (2002). A physiologically based pharmacokinetic and pharmacodynamic (PBPK/PD) model for the organophosphate insecticide chlorpyrifos in rats and humans. *Toxicol. Sci.* **66,** 34–53.

Van den Beukel, I., Dijcks, F. A., Vanderheijden, P., Vauquelin, G., and Oortgiesen, M. (1997). Differential muscarinic receptor binding of acetylcholinesterase inhibitors in rat brain, human brain and Chinese hamster ovary cells expressing human receptors. *J. Pharmacol. Exp. Ther.* **281,** 1113–1119.

Ward, T. R., Ferris, D. J., Tilson, H. A., and Mundy, W. R. (1993). Correlation of the anticholinesterase activity of a series of organophosphates with their ability to compete with agonist binding to muscarinic receptors. *Toxicol. Appl. Pharmacol.* **122,** 300–307.

Winrow, C. J., Hemming, M. L., Allen, D. M., Quistad, G. B., Casida, J. E., and Barlow, C. (2003). Loss of neuropathy target esterase in mice links organophosphate exposure to hyperactivity. *Nat. Genet.* **33,** 477–485.

Zhao, Z., Rothery, R. A., and Weiner, J. H. (1999) Stopped flow studies of the binding of 2-*n*-heptyl-4-hydroxyquinoline-*N*-oxide to fumarate reductase of *Escherichia coli*. *Eur. J. Biochem.* **260,** 50–56.

Zwart, R., and Vijverberg, H. P. M. (1997). Potentiation and inhibition of neuronal nicotinic receptors by atropine: Competitive and non-competitive effects. *Mol. Pharmacol.* **52,** 886–895.